Core–Shell Structured Latex Particles. II. Synthesis and Characterization of Poly(*n*-butyl acrylate)/Poly(benzyl methacrylate–styrene) Structured Latex Particles

I. SEGALL,[1,*] V. L. DIMONIE,[1] M. S. EL-AASSER,[1,†] P. R. SOSKEY,[2] and S. G. MYLONAKIS[2]

[1]Emulsion Polymers Institute, 111 Research Dr., Iacocca Hall, Lehigh University, Bethlehem, Pennsylvania 18015; [2]EniChem America Inc., Research and Development Center, 2000 Cornwall Rd., Monmouth Junction, New Jersey 08852

SYNOPSIS

The synthesis of structured latex particles involved the preparation of a slightly crosslinked poly(*n*-butyl acrylate) (PBA) seed and a poly(benzyl methacrylate–styrene) [P(BM–St)] shell. It was found that structured core–shell latex particles prepared by semicontinuous monomer addition yielded better coverage of the seed particles than those polymerized by batch and that poly(benzyl methacrylate) yielded better coverage than polystyrene (PS). Polymerizations in the presence and absence of a chain transfer agent indicated that the presence of isooctyl mercaptopropionate (IOMP) causes the second-stage monomer to polymerize as an isolated, single patch of shell material. In the absence of IOMP, smaller patches of shell material are spread throughout the PBA seed surface. The different morphologies obtained under different polymerization conditions were attributed to thermodynamic and kinetic factors such as polymer–polymer interfacial tensions and viscosity effects. © 1995 John Wiley & Sons, Inc.

INTRODUCTION

The purpose of this study (the second in a series of three) is to describe the synthesis and characterization of poly(*n*-butyl acrylate)/poly(benzyl methacrylate–styrene) structured latexes designed specifically for the modification of polycarbonate matrix. The results of the use of these core–shell latex systems in toughening polycarbonate will be the subject of the third paper in this series.

Structured latex particles can be produced by emulsion polymerization in more than one way.[1–8] In seeded or multistage methods a monomer or monomer mixture is polymerized in the presence of preformed latex particles which are used as seed.[5,9–19] The seeded emulsion polymerization allows preparation of a wide range of structured latex particles with varied morphologies, ranging from homogeneous radial composition to core–shell particles with boundary layers with a thickness in the nanometer range. Core–shell latex particles can be used as impact modifiers where the rubbery core imparts ductility or undergoes some cavitation while the glassy shell provides anchorage and miscibility with the matrix.

It was demonstrated[15,20–28] that thermodynamic and kinetic factors dictate the particle morphology of structured latexes. These two competing factors affect the polymerization process and the final morphology of structured latex particles in a complex manner. The thermodynamic factors determine the stability of the ultimate particle morphology in accordance with minimization of the surface free-energy change.[20,29] The polymer which has a lower interfacial tension against the water phase will tend to stay on the surface, decreasing the total free energy. The second factor is related to the kinetics of the morphological development by the diffusion rate of the components of the system. Factors such as the viscosity at the polymerization loci and the mode of monomer addition determine the ease by which thermodynamically preferred morphology can be achieved.[30]

* Present address: University of Cincinnati, Department of Materials Science & Engineering, Cincinnati, OH 45221.
† To whom correspondence should be addressed.

Journal of Applied Polymer Science, Vol. 58, 401–417 (1995)
 CCC 0021-8995/95/020401-17

Based on these fundamental concepts, the polymerization process parameters were screened and selected to permit the synthesis of structured latex particles with the designed particle morphology.

The characterization of structured latex particles[31-37] is of eminent importance not only in understanding the mechanisms underlying the polymerization process but also in defining the bulk and surface properties of the particles[38] and the phase separation.[39-44] Min et al.[45] discovered that the morphological stability of core–shell latex particles depends on the amount of graft copolymer formed during the seeded emulsion polymerization.

MATERIALS

Poly(*n*-butyl acrylate) (PBA) latex particles, small and large, with variable amounts of ethylene glycol dimethacrylate (EGDMA) crosslinker, synthesized as described elsewhere[46] and detailed in Part I of this series, were used for the seeded emulsion polymerization. Benzyl methacrylate (BM, Polysciences Inc.) and 2,2,3,3,4,4,5,5-octafluoro-hexanediol 1,6 dimethacrylate (FDMA, Monomer-Polymer and Dajac Laboratories, Inc.) monomers were passed through an inhibitor remover column equipped with inhibitor removal packing material designed to remove hydroquinone (HQ) and methyl ether hydroquinone (MEHQ) (Aldrich). Potassium persulfate initiator ($K_2S_2O_8$), FMC, and isooctyl mercaptopropionate chain transfer agent (IOMP, Evans Chemetics Co.) were used as received. Water was distilled and deionized.

EFFECT OF SECOND-STAGE MONOMER ADDITION MODE ON LATEX PARTICLE MORPHOLOGY

Core–shell latexes were prepared using the 93/7 poly[(*n*-butyl acrylate)/crosslinker] (PBA/EGDMA) weight ratio seed latex particles of 184 nm in diameter, prepared according to the procedure given earlier. Benzyl methacrylate was used as the second-stage monomer. Batch and semicontinuous monomer addition modes at different feed rates were used in order to establish the polymerization parameters needed for best coverage of the PBA rubbery core particles by the poly(*n*-benzl methacrylate) (PBM) glassy second-stage polymer. The polymerizations were carried out at 70°C under a N_2 blanket, in a 25-mL Erlenmeyer flask equipped with a magnetic stirrer. The basic recipe is given in Table I.

The morphology of the resulting latexes was studied by transmission electron microscopy (TEM) using preferential staining techniques. Figure 1 presents a series of electron micrographs of core–shell latexes which were taken after negative staining with uranyl acetate (UAc, to increase the contrast between the background and the particles), and preferential staining with ruthenium tetroxide (RuO_4, to differentiate the rubbery from the glassy phases). Figure 1(A) shows a core–shell latex prepared by batch polymerization where the PBA seed particles (lighter phase) appear to be only partially covered by the PBM second-stage (darker phase) polymer. Figures 1(B), 1(C), and 1(D) show that PBA–PBM latexes prepared by semicontinuous addition at different feed rates of the BM second-stage monomer and at several initiator concentrations yielded a better, though not complete, coverage of the seed latex particles. The samples shown in Figures 1(B) and 1(C) were prepared by adding the second-stage monomer at the same feed rate (i.e., 1.08 mL/h), with sample 1(C) containing twice the amount of initiator used for the second-stage polymerization. Sample 1(D) was synthesized by using a slower feed rate (i.e., 0.54 mL/h) while keeping the initiator concentration at the same level as that shown for Figures 1(A) and 1(B). The micrographs are not conclusive as to the effect of the BM monomer feed rate and amount of initiator used for the second-stage polymerization on the extent of coverage of the PBA seed by the PBM second-stage polymer.

A careful examination of the micrographs reveals that there is no second crop of particles formed. Some portion of each structured particle is more uniformly covered by the second-stage PBM polymer, while other parts exhibit polymer "lumps," as if the seed PBA particles were covered by a PBM "shell" with variable thickness.

By comparing the structured latex particles prepared by batch polymerization [Fig. 1(A)] with all

Table I Recipe for the Preparation of Core–Shell PBA/PBM Latex Particles

Component	Amount (g)
PBA seed latex[a]	3.0 (25% solids)
DDI water	6.7
Potassium persulfate	0.024
Benzyl methacrylate	2.4
IOMP	0.0024

[a] 184 nm in diameter.

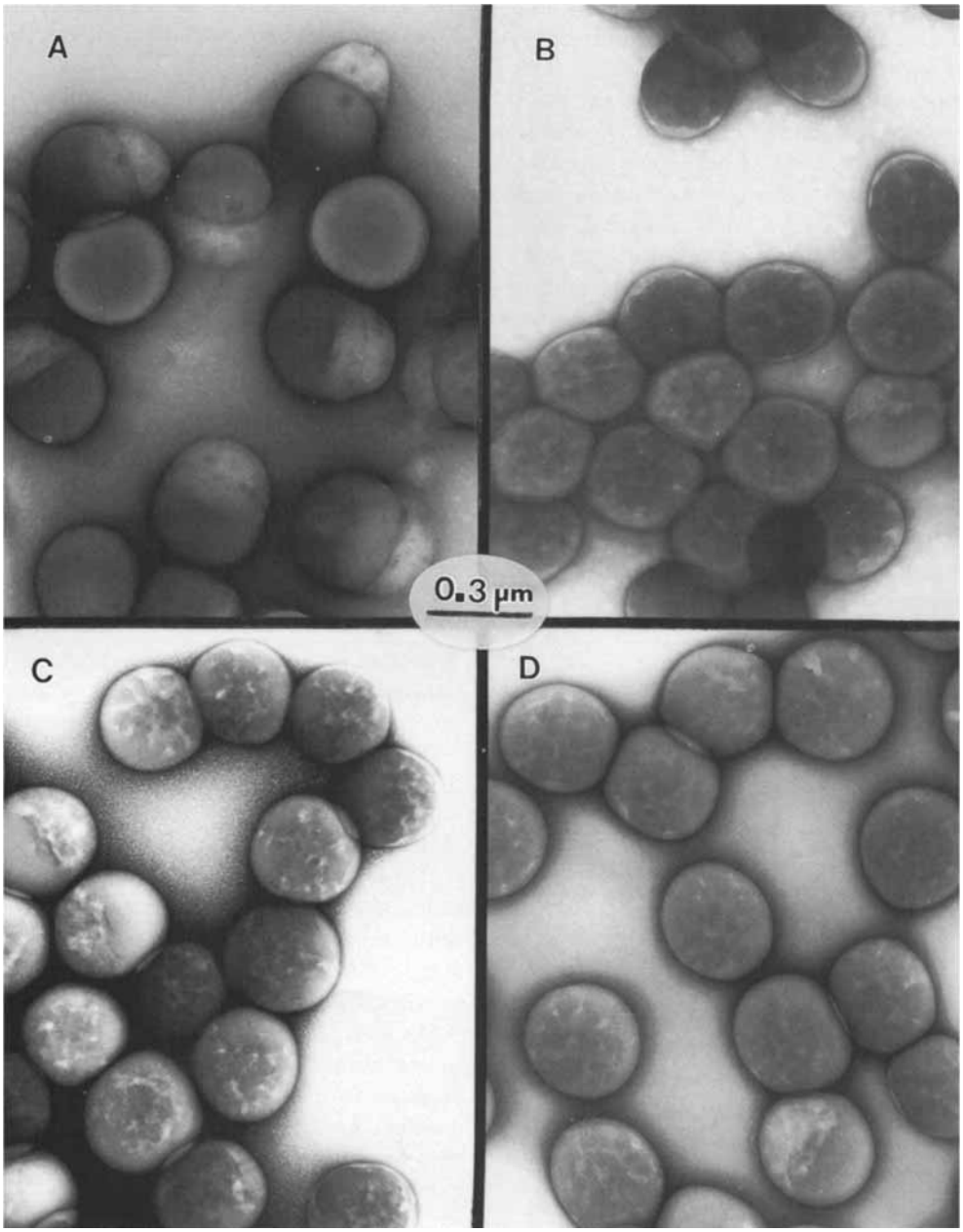

Figure 1 Transmission electron micrographs of core–shell PBA–PBM latexes prepared by seeded emulsion polymerization via (A) batch polymerization, (B) semicontinuous polymerization (1.08 mL/h), (C) semicontinuous polymerization (1.08 mL/h, with twice the amount of initiator used for the second-stage polymerization), and (D) semicontinuous polymerization (0.54 mL/h). Lighter regions = PBA, darker regions = PBM.

the structured latex particles synthesized via semicontinuous polymerization [Figures 1(B), 1(C), and 1(D)], it is clear that the mode of second-stage monomer addition is highly influential in determining the morphology of two-stage latex particles. In a batch second-stage polymerization process, where all the monomer is added to the first-stage seed particles at the outset of the reaction, relatively high levels of second-stage monomer are present initially. These monomer molecules have much greater freedom to diffuse than macromolecules. Moreover, the presence of monomer molecules inside the first-stage particles enhances the mobility of the first-stage polymer molecules such that migration of these

molecules is also more likely, and phase separation may occur to satisfy thermodynamic equilibrium conditions. In contrast, when semicontinuous polymerization methods are employed, where the second-stage monomer is added gradually to the first-stage seed particles, the level of monomer concentration at any time during the polymerization can be kept to a minimum (i.e., monomer-starved feed conditions). In this process, the second phase will be present primarily in the form of polymer molecules which are relatively hindered in their mobilities as compared with monomer molecules. Therefore, the semicontinuous polymerization process (under starved conditions) imposes a higher kinetic barrier for the diffusion of the second-stage polymer, and the resulting polymerization is less site selective. Based on these results, semicontinuous polymerization was used throughout the course of this work in order to ensure better distribution of the shell polymer on the rubber core latex particles.

SMALL-SIZE STRUCTURED LATEX PARTICLES

Structured latex particles with a calculated shell layer thickness of 50 or 25 nm were synthesized using seeded emulsion polymerization according to the recipes given in Tables II and III, respectively. Monodisperse PBM latex with particle diameter of 180 nm, with two different crosslinker levels of 1 or 7%, were used as seed. Of the total benzyl methacrylate monomer 15% was used for swelling the seed particles. The swelling was carried out with stirring, at the polymerization temperature of 70°C, over a period of 20 min. The rest of the monomer was mixed with IOMP chain transfer agent and fed into a 500-mL round-bottom reaction flask equipped with a reflux condenser, mechanical stirrer, nitrogen inlet tube, and a monomer addition pump. Feed rates of 13.5 and 16.35 mL/h were chosen for the addition

Table II Recipe for the Preparation of Thick-Shell (50 nm) Structured Latex Particles

Component	Amount (g)
P(BA/EGDMA) seed latex (25% solids)	75
DDI water	150
Monomer (variable BM/St ratio)	52
IOMP	1 wt %[a]
Potassium persulfate	0.52

[a] Based on amount of monomer fed continuously.

Table III Recipe for the Preparation of Thin-Shell (25 nm) Structured Latex Particles

Component	Amount (g)
P(BA/EGDMA) seed latex (25% solids)	150
DDI water	120
Monomer (variable BM–St ratios)	41
IOMP	0.7 or 1 wt %[a]
Potassium persulfate	0.41

[a] Based on monomer fed continuously.

of the second-stage monomer to produce "thick" (T, 50 nm) and "thin" (t, 25 nm) polymer shell layers, respectively. Polymerizations were carried at 70°C to yield core–shell weight ratios of 1 : 2.77 and 1 : 1.09 for the thick and thin shell layers, respectively.

Particle Size Analysis

A total of seven structured latexes were prepared by varying the EGDMA crosslinker concentration, the amount and type of second-stage monomer, and the IOMP chain transfer agent concentration. Table IV lists the variables involved in the preparation of each one of the seed latexes as well as the structured latexes.

Table IV also shows the particle size and the particle size polydispersity index (PDI = D_w/D_n) as obtained from TEM micrographs (using the cold-stage holder), as well as from the Nicomp submicron particle sizer.

As seen in Table IV, there is no consistent trend in correlation between TEM and Nicomp particle sizes as to which latex particles have a larger diameter. Samples 220 and 221 were thick-shell samples for which a 100-nm increase in diameter was expected. The particle sizes for the structured latex samples 220 and 221, were 280 and 223 nm, respectively (based on TEM data), starting from a 180-nm seed size. Sample 220 had 7% EGDMA crosslinker in the seed while sample 221 had only 1% crosslinker. An increase in the amount of crosslinker might decrease the interstitial space and prevent the diffusion of the second-stage monomer into the seed particles and, therefore, yield larger particles. For thin-shell particles (samples 222 and 223), there was no significant size difference resulting from the degree of crosslinking of the PBA seed, since there was not much monomer available for diffusion into the seed particles to cause a noticeable change.

Samples 224 and 225 had a shell layer composition of 95/5 poly(benzyl methacrylate–styrene)

Table IV Particle Composition and Size Analysis of a First Series of Structured Latex Particles

Sample	Seed Latex BA/EGDMA Wt Ratio	Shell Layer Thickness[a]	Shell Layer Composition Wt Ratio	IOMP Wt %[b]	Nicomp		TEM	
					D_v[c] (nm)	Coefficient Variation (%)	D_w[d] (nm)	PDI (D_w/D_n)
Seed particles								
108	93/7	—	—	—	177	26	187	1.03
109	99/1	—	—	—	158	9	176	1.04
Structured particles								
220	93/7	*T*	100 BM	1.0	331	29	280	1.02
221	99/1	*T*	100 BM	1.0	331	29	223	1.02
222	93/7	*t*	100 BM	1.0	250	27	227	1.03
223	99/1	*t*	100 BM	1.0	180	33	220	1.03
224	99/1	*t*	95/5 BM/St	1.0	186	26	208	1.04
225	99/1	*t*	95/5 BM/St	0.7	191	26	209	1.04
226	99/1	*t*	100 St	0.7	200	22	181	1.02

[a] *T*, thick shell (ca. 50 nm); *t*, thin shell (ca. 25 nm); calculations are based on 180-nm seed particle diameter.
[b] Based on the amount of continuously fed second-stage monomer.
[c] Volume-average diameter.
[d] Weight-average diameter (over 500 particles were counted off electron micrographs).

P(BM–St), as opposed to the 100% PBM in the shells of samples 220–223. The density difference due to changes in the composition of the second-stage monomer is not expected to affect the shell layer thickness significantly. Sample 225 had less IOMP chain transfer agent (0.7 wt %, based on monomer fed continuously) than sample 224 (1 wt %), this difference did not seem to have an effect on the particle size. Overall, the particle diameters were smaller than expected (208 and 209 nm instead of the theoretical value of 230 nm). The shell composition of sample 226 was 100% polystyrene. The final size of the particles according to TEM analysis was practically the same as that for the seed particles. However, TEM pictures did not show the presence of a secondary crop of particles.

The preparation of an additional series of seed and structured latexes was carried out in order to check on the reproducibility of the polymerization process. Tables IV and V list the composition and corresponding particle size as obtained from electron microscopy, Nicomp submicron particle sizer, and capillary hydrodynamic fractionation (CHDF–1100 particle size analyzer, MATEC) analysis (sample numbers 118, 119, and 230–236 correspond to the original series 108, 109, and 220–226, respectively).

The weight and number-average particle sizes obtained for samples 230, 231, and 232 were within the range obtained by TEM and Nicomp analysis, as indicated in Table V. With all three measuring techniques it was observed that latex sample 230 yielded a larger size than samples 231 and 232. The CHDF results substantiated the belief that 1% crosslinked PBA seed latex particles were indeed smaller than those of 7% crosslinked PBA seed latex.

MORPHOLOGY STUDIES OF STRUCTURED LATEX PARTICLES

Morphology studies of the structured latex particles were performed by TEM on samples stained with UAc followed by RuO_4 vapors. Figure 2 shows the transmission electron micrographs of PBA–PBM with a thick PBM shell [Fig. 2(A)] and a thin PBM shell [Fig. 2(B)]. Figure 2 also allows for the comparison of the morphology differences due to the shell polymer composition; PBM [in 2(B)], P(BM–St) [in 2(C)], and PS [in 2(D)].

Micrographs of the 230–236 structured latex particles series show the same characteristic morphology as the 220–226 series; namely, better coverage for the PBA seeds with the PBM shell, patches for the PBA seeds covered with the P(BM–St) shell, and almost complete phase separation for the PBA seeds "covered" with the 100% PS "shell." These facts indicate the tendency of polystyrene to phase separate from PBA due to larger polymer–polymer interfacial tensions, while PBM has a higher affinity for the PBA seed particles.

Additional structured latex particles (samples 250 and 251) were synthesized according to the basic

Table V Composition and Particle Size Analysis of a Second Series of Structured Latex Particles

					Nicomp		TEM		CHDF	
Sample	Seed BA/EGDMA Wt Ratio	Shell Thickness[a]	Shell Comp. Wt Ratio	IOMP Wt %[b]	D_v[c] (nm)	Coefficient Variation (%)	D_w[d] (nm)	PDI (D_w/D_n)	D_w (nm)	PDI
Seed particles										
118	93/7	—	—	—	204	6	192	1.01	203	1.03
119	99/1	—	—	—	164	20	185	1.02	173	1.04
Structured particles										
230	93/7	*T*	100 BM	1.0	317	21	268	1.01	285	1.00
231	99/1	*T*	100 BM	1.0	249	27	225	1.02	248	1.01
232	93/7	*t*	100 BM	1.0	244	22	233	1.01	240	1.01
233	99/1	*t*	100 BM	1.0	200	18	188	1.02	—	—
234	99/1	*t*	95/5 BM-St	1.0	171	32	181	1.02	—	—
235	99/1	*t*	95/5 BM-St	0.7	199	24	195	1.02	—	—
236	99/1	*t*	100 St	0.7	175	34	186	1.03	—	—

[a] *T*, thick shell (ca. 50 nm), *t*, thin shell (ca. 25 nm), based on 180-nm seed particle diameter.
[b] Based on the amount of continuously fed second-stage monomer.
[c] Volume-average diameter.
[d] Weight-average diameter (over 500 particles counted off TEM micrographs).

recipe given in Table III, using the 1 wt % crosslinked 180 nm in diameter PBA seed latex. The rest of the BM monomer was fed semicontinuously, as before, at a feed rate of 16.35 mL/h, in the absence of IOMP chain transfer agent (CTA). Table VI lists the variables in the polymerization parameters.

Samples 250 and 251 were both synthesized at a 1/1 core–shell weight ratio in the absence of IOMP. In the case of sample 250, all of the initiator was added at the end of the 20-min swelling period of the PBA seed latex with 15% of the second-stage BM monomer, when the continuous addition of the remaining BM began. In the case of sample 251, a solution of initiator dissolved in distilled-deionized (DDI) water was added continuously, over a period of 90 min, starting at the same time as the continuous feed of the BM second-stage monomer. Micrographs of samples 250 and 251, negatively stained with UAc and preferentially stained with RuO_4, are shown in Figure 3. There is no appreciable difference in the morphology of these two samples that could be attributed to the difference in the initiator addition mode.

In order to produce even "thinner shell" in the structured latex particles, the recipe shown in Table VII was used. The BM second-stage monomer was fed semicontinuously; 15% of it was used for the swelling of the PBA seed latex particles (1 wt % crosslinker, 180 nm) at the polymerization temperature of 70°C, and the remainder was fed at an addition rate of 0.29 mL/min.

Table VI lists the variables in the polymerization parameters. Samples 252 and 253 had a core–shell weight ratio of 1/0.435 (lower PBM second-stage polymer than in samples 250 and 251). The BM second-stage monomer was added to the PBA seed latex neat (252) or mixed with IOMP (253). The resulting difference in the particle morphology due to the absence or presence of IOMP can be seen in Figure 4. Sample 252, prepared in the absence of IOMP had small patches of PBM spread all over the surface of the PBA seed particles. Sample 253, prepared in the presence of IOMP had larger patches, concentrated in fewer locations throughout the surface of the seed particles. These morphologies are attributed to the combined kinetic and thermodynamic effects. The presence of a CTA reduces the molecular weight of the second-stage polymer chains and hence the viscosity, lowering the kinetic barrier and favoring polymer chain diffusion to achieve a thermodynamic state of lower free energy for the system.

LARGE-SIZE STRUCTURED LATEX PARTICLES

It is of interest to measure the toughening of a polycarbonate (PC) matrix by structured latex particles of different sizes in order to determine if there is an optimum particle size for the enhancement of impact resistance.

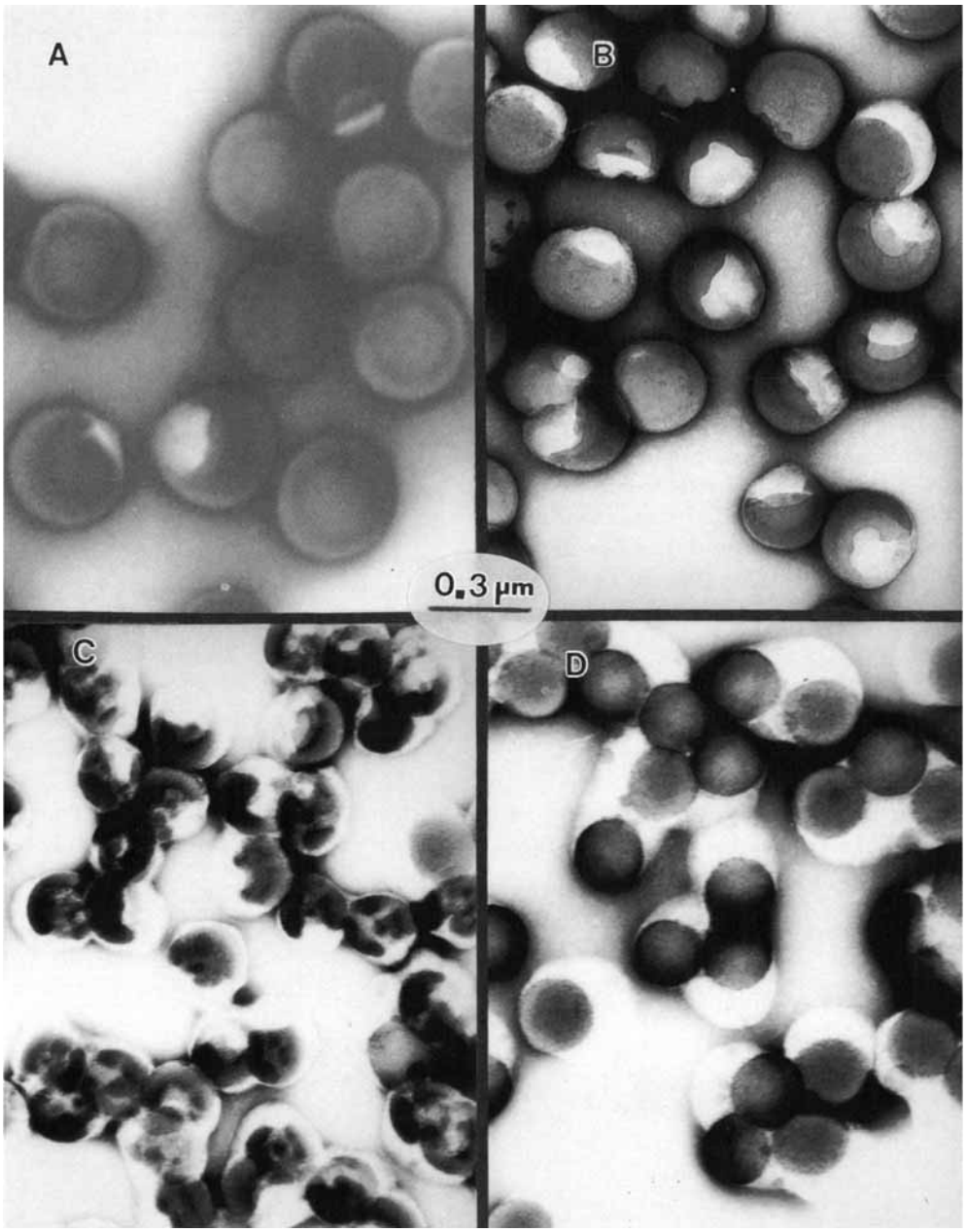

Figure 2 Transmission electron micrographs of samples stained with UAc and RuO_4. (A) core–shell PBA–PBM thick-shelled latex (sample 220), (B) core–shell PBA–PBM thin-shelled latex (sample 222), (C) PBA/P(BM–St) latex particles (sample 224), and (D) PBA–polystyrene latex particles (sample 226). Lighter regions = PBA, darker regions = PBM, P(BM–St), or polystyrene.

Larger PBA seed latex particles, of 350 nm diameter (compared to 180 nm discussed thus far), were synthesized as described earlier[46] and in the first part of this series, at a 99/1 BA–EGDMA weight ratio. The basic recipe for the synthesis of structured latex particles using the large seed latex particles is given in Table VIII. The second-stage polymerization was carried out under the same conditions as for smaller PBA seeds, the second-stage feed rate was 0.612 mL/min in the absence of a chain transfer agent. The core–shell composition and theoretical shell thickness of these large-size structured latex particles are given in Table IX.

Table VI Variables in the Polymerization Parameters of the PBA–PBM 250 Series

Sample	Core/Shell Wt Ratio	Shell Thickness (nm)[a]	CTA (IOMP)	Initiator Feed[b]
250	1/1	22	No	—
251	1/1	22	No	Continuously
252	1/0.435	11	No	—
253	1/0.435	11	Yes	—

[a] Calculated based on 180-nm seed particle diameter.
[b] Initiator added all at once unless otherwise specified.

Morphology Studies of Large-Size PBA–PBM Structured Latex Particles

TEM micrographs showing the morphology of PBA–PBM large-size structured latex particles can be seen in Figure 5. As the amount of second-stage monomer added to the system was increased, the size of the PBM patches spread over the surface of PBA seed grew.

EXTENT OF PBA SEED COVERAGE BY THE PBM SECOND-STAGE POLYMER

The quantitative interpretation of the degree of coverage of the seed particles by the second-stage polymer is very difficult to obtain from TEM observation. Other techniques were sought.

Crosslinked PBA seed latex particles were synthesized at a 93/7 (BA/FDMA) weight ratio (FDMA is a fluorinated crosslinker). The crosslinked PBA latex particles (150 nm in diameter) were used as the seed particles for a series of polymerizations. BM was used as the second-stage monomer. The second-stage polymerizations were carried out at 70/30 and 30/70 PBA–PBM weight ratios, according to the recipe given in Table VIII, by various polymerization processes: batch, semicontinuous in the presence of IOMP chain transfer agent, and semicontinuous in the absence of CTA. Figure 6 gives the TEMs of the structured latex particles, negatively stained with UAc, and subse-

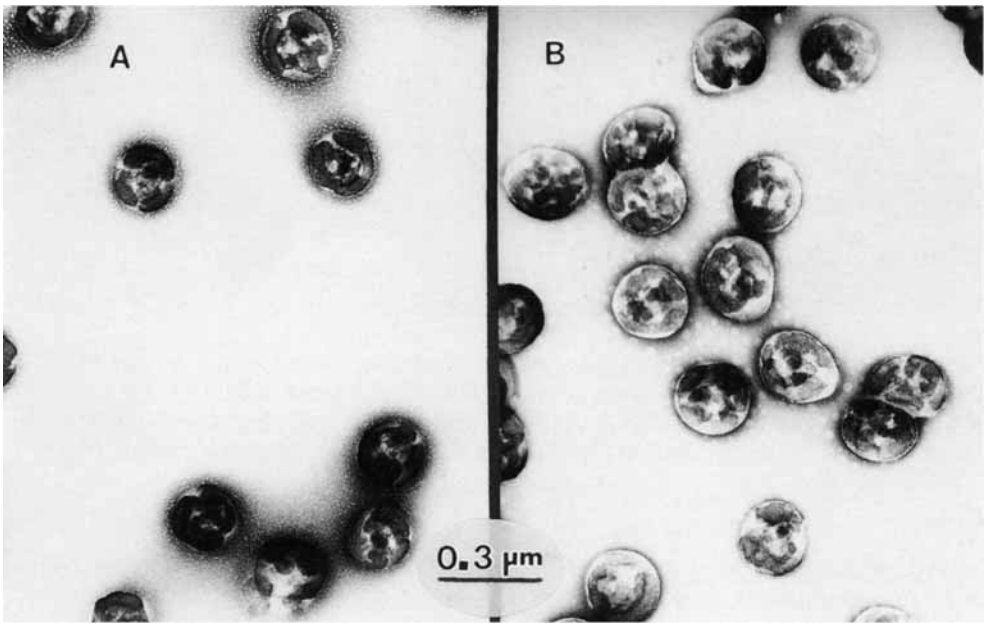

Figure 3 Transmission electron micrographs of 1/1 core–shell latex particles stained with UAc and RuO_4. Core is 1% crosslinked PBA. Shells are PBM synthesized in the absence of chain transfer agent. (A) Initiator is fed at once and (B) initiator is fed continuously. Lighter regions = PBA, darker regions = PBM.

Table VII Recipe for the Preparation of Very Thin Shells (11 nm) Structured Latex Particles

Component	Amount (g)
P(BA/EGDMA) seed latex (25% solids)	150
DDI water	63
Benzyl Methacrylate	16
IOMP	0.7 wt %[a]
Potassium persulfate	0.27

[a] Based on monomer fed continuously.

Table VIII Basic Recipe for the Synthesis of Large-Size PBA–PBM Structured Latex Particles

Component	Amount (g)
Seed latex (PBA 41 + 42 mix)[a]	500 (25% solids)
Benzyl methacrylate	Variable (6 to 29)
Potassium persulfate	1 wt %[b]
DDI water	2–4 mL

[a] Weight-average particle diameter = 350 nm.
[b] Based on benzyl methacrylate monomer.

quently preferentially stained with RuO_4. The top three micrographs correspond to thin-shell structured latex particles with a PBA–PBM weight ratio of 70/30. The bottom three micrographs correspond to thick-shell structured latex particles with a 30/70 PBA–PBM weight ratio. For both the top and bottom rows, from left to right, the polymerization process employed for the synthesis of the structured latex particles was batch, semicontinuous in the presence of CTA, and semicontinuous in the absence of CTA. Comparing the top and bottom rows, it can be seen that at lower core–shell ratios (bottom row, thicker shell), more surface area of the PBA seed latex particles was covered by the second-stage polymer. On the top row, going from left to right, it is observed that batch polymerization of the second-stage monomer led to second-stage polymer at isolated points on the surface of the PBA seed, while semicontinuous addition of the second-stage monomer resulted in small patches of PBM polymer spread over the surface of the PBA seed particles. On the bottom row, where the amount of second-stage polymer is larger than on the top row, it becomes hard to distinguish morphology differences as a function of the polymerization process.

Extent of Core Particle Coverage Determined by Fluorine Concentrations in Tagged Structured Latex Particles

Electron spectroscopy for chemical analysis (ESCA), which enables the user to analyze the

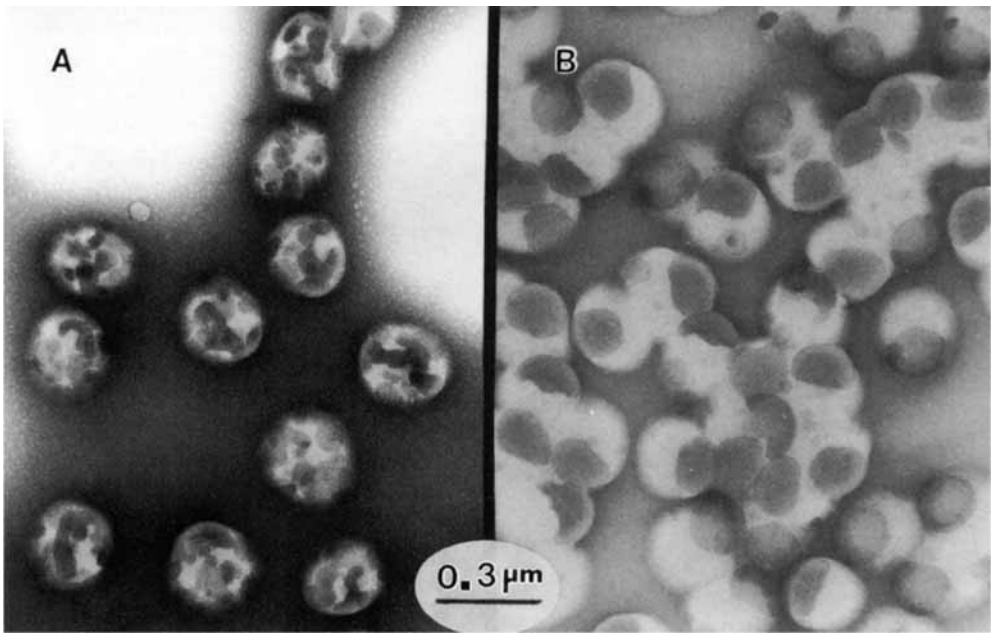

Figure 4 Transmission electron micrographs of 1/0.435 core–shell latex particles stained with UAc and RuO_4. Core is 1% crosslinked PBA. Shells are PBM synthesized: (A) in the absence of chain transfer agent, and (B) in the presence of chain transfer agent. Lighter regions = PBA, darker regions = PBM.

Table IX Composition and Theoretical Shell Thickness for PBA–PBM Large-Size Structured Latex Particles

Sample	PBA–PBM Wt Ratio	Theoret. Shell Thickness[a] (nm)
261	1/0.060	3
262	1/0.123	7
263	1/0.256	14
264	1/0.357	18

[a] Based on 350 nm PBA seed particle diameter (obtained by CHDF analysis.)

chemical nature of the surface up to 100 Å deep,[47,48] indicated that fluorine/carbon (F/C) ratio for the seed (3.6/96.4) was higher than the F/C ratio for any of the structured latex particles, as expected, since the second stage, PBM, did not contain any of the tagged material (fluorinated crosslinker). All of the structured latex particles exhibited a fluorine concentration between 1.5 and 2.1%. The fluorine content difference from one structured latex sample to the next was not significant enough to draw conclusions regarding the extent of coverage of the PBA tagged seed by the PBM shell. The PBA coverage by the PBM was not continuous or of a uniform thickness, so the PBA seed could be seen through. Therefore, in order to better evaluate the extent of coverage based on tagging, large enough amounts of BM are required for the so-called thick shell to exhibit complete coverage of the PBA seed particles.

Extent of Core Particle Coverage Determined by Carbon–Oxygen Bearing Carbon Ratio of Structured Latex Particles of Various Core–Shell Weight Ratios

It is common knowledge that the presence of oxygen atoms has a profound effect on the binding energies of the respective carbon atoms, and hence the C(1*s*) signal in ESCA spectrum changes dramatically with polymer composition. The chemical structure of BA, BM, and FDMA, depicting the different carbon bondings is shown in Figure 7. It can be seen from Figure 7 that there are mainly three types of carbon atoms present in the system. The backbone carbon atom is represented as C^a and has a binding energy of 285 eV. The COO carbon atom is represented as C^b and has a binding energy of 289 eV, and the CO carbon atom, represented as C^c, posses a binding energy of 287 eV. It can also be seen from Figure 7 that the ratio of carbons to oxygen bearing carbons (C/CO) for each one of the monomers comprising the system is different. Figure 8 is an X-ray photoelectron spectrum of the carbon [C(1*s*)] peak for a core–shell latex system indicating the shift in binding energy due to oxygen bonding. The fractional areas corresponding to carbons bonded to hydrogens and other carbons and oxygen bearing carbons can be determined from the deconvoluted X-ray photoelectron spectra.

Table X contains a list of theoretical carbon–oxygen bearing carbon ratios as well as experimental values for different samples as a function of shell thickness and polymerization process and conditions. It can be seen that for a given core–shell ratio (thin shell or thick shell), the C/CO ratio decreases when changing the polymerization process from batch to semicontinuous in the presence of CTA to semicontinuous in the absence of CTA. One can correlate these results with the particle morphology given in Figure 6. One can follow the morphological transition from extended phase separation, with a few thick patches of shell material in the case of batch polymerization [Fig. 6(A)], to a large number of smaller sized patches of shell material in the semicontinuous polymerization [Figures 6(B) and 6(C)]. For a given polymerization process (batch, semicontinuous with CTA, or semicontinuous without CTA), the C/CO ratio decreases as the shell thickness decreases, since more of the seed which contains a higher concentration of CO is exposed (see micrographs in Fig. 6 and compare bottom row for thick-shell latexes to top row for thinner shell latexes).

GLASS TRANSITION TEMPERATURES

Differential Scanning Calorimetry Analysis

Differential scanning calorimetry (DSC) analysis was performed on dried latex samples as described earlier.[46] Figure 9 is the plot of the derivative of a DSC scan of three samples of structured latex particles. All three samples were synthesized with 1 wt % crosslinked PBA seed and differ in their shell compositions. Curve *A* corresponds to the PBA–PBM (sample 223), curve *B* corresponds to the PBA/P(BM–St) (sample 225), and curve *C* corresponds to the PBA–PS (sample 226) structured latex particles. Table XI contains the detailed composition of these samples. It can be seen in Figure 9 that the curves of all three samples have a first minimum at approximately −45°C, the glass transition temperature (T_g) corresponding to the 1 wt % crosslinked PBA seed (see Table XI, sample 109). The second

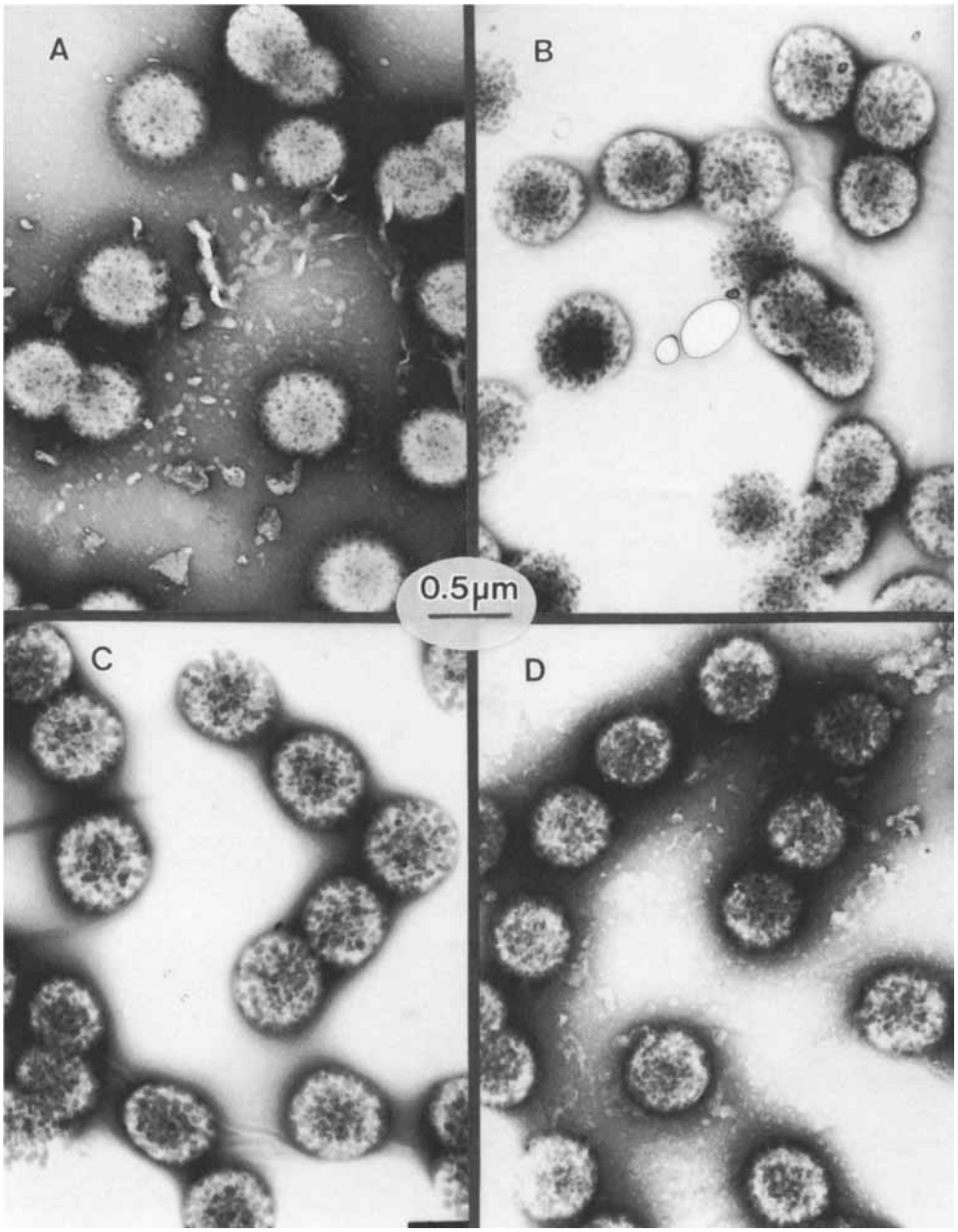

Figure 5 Transmission electron micrographs of structured latex particles stained with UAc and RuO_4. Core is 1% crosslinked PBA, 350 nm in diameter; shells are PBM; core–shell weight ratios are: (A) 1/0.060, (B) 1/0.123, (C) 1/0.256, and (D) 1/0.357. Lighter regions = PBA, darker regions = PBM.

T_g, due to the shell polymer of each one of these structured latex samples, appears at a different temperature; 61, 70, and 101°C, corresponding to 100% PBM, 95/5 P(BM–St), and 100% PS shell compositions, for curves *A, B,* and *C,* respectively. The intermediate T_g observed around −5°C on curve *B* indicates transition domains where PBA and P(BM–St) copolymer are not phase separated. The seed sample 108 had 7% crosslinker, and therefore a higher T_g (−40°C) than the seed latex sample 109 (−45°C) which contained only 1% crosslinker, allowing for more chain motion. All structured latex particles showed two glass transition temperatures, one for the core material and one for the shell material. The latex with a 100% PS shell layer (sample 226) exhibits a T_g of 101°C, as expected for poly-

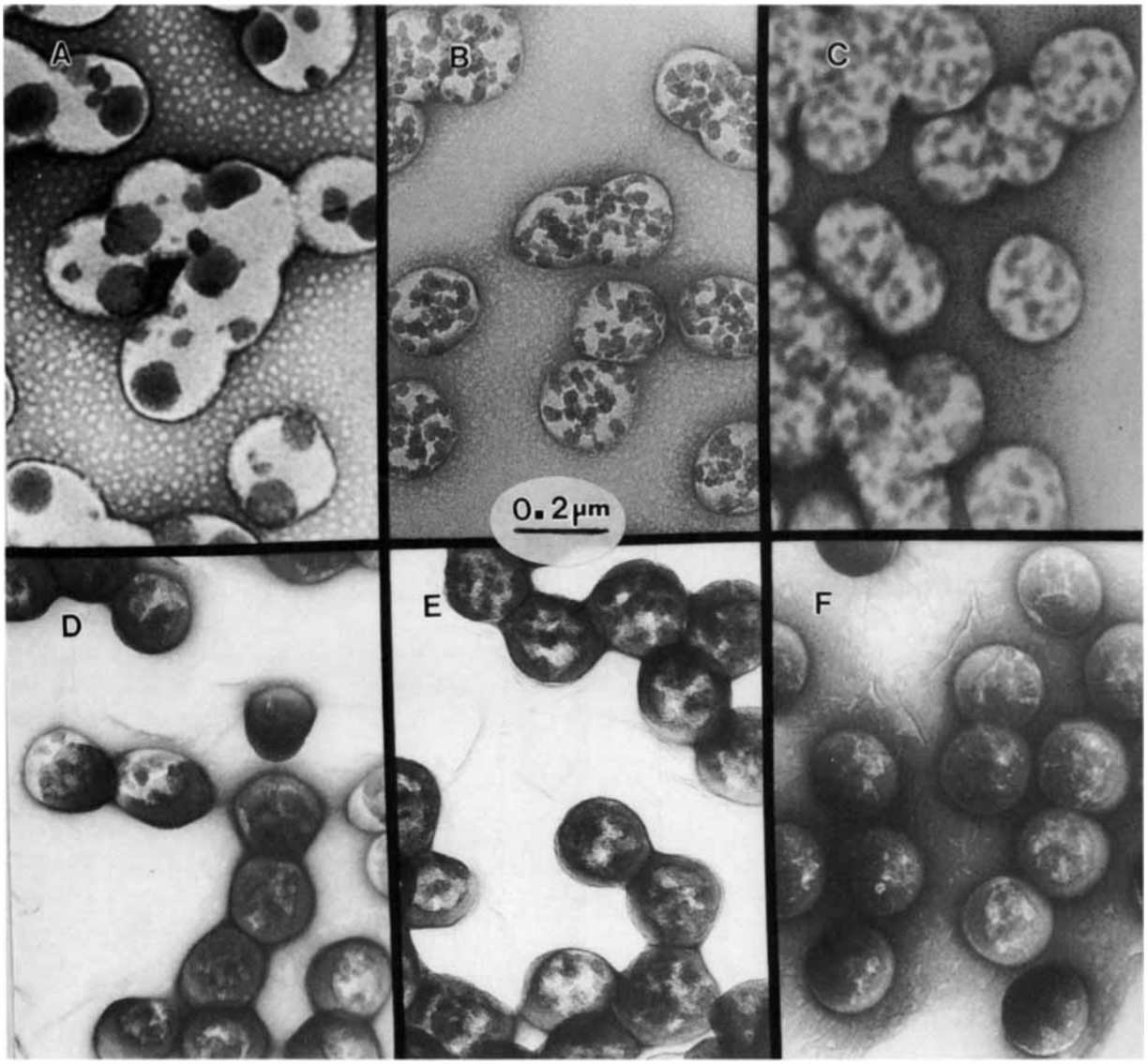

Figure 6 Transmission electron micrographs of core–shell latex particles stained with UAc and RuO_4. Top: 70/30 core–shell weight ratio; core is 93/7 P(BA–FDMA); shell is PBM produced by: (A) batch polymerization, (B) semicontinuous polymerization in the presence of a chain transfer agent, and (C) semicontinuous polymerization in the absence of a chain transfer agent. Bottom: 30/70 core–shell weight ratio; core is the same as on the top series, shells are PBM synthesized by: (D) batch polymerization, (E) semicontinuous polymerization in the presence of a chain transfer agent, and (F) semicontinuous polymerization in the absence of a chain transfer agent. Lighter regions = PBA, darker regions = PBM.

styrene. Samples with shell compositions of 95/5 P(BM–St) (samples 224 and 225) show T_g values of 67 and 70°C when using higher and lower IOMP chain transfer agent concentrations, respectively, indicating higher mobility and lower glass transition temperature for the sample with shorter chains (molecular weight effect). These two samples present some intermediate peaks indicating transition domains where PBA and P(BM–St) copolymer are not phase separated.

Samples 220 and 221 (thick shells) have greater areas under the curves of the heat flow derivative for the glassy polymer compared to the rubbery polymer, corresponding to the roughly 1 : 3 PBA–

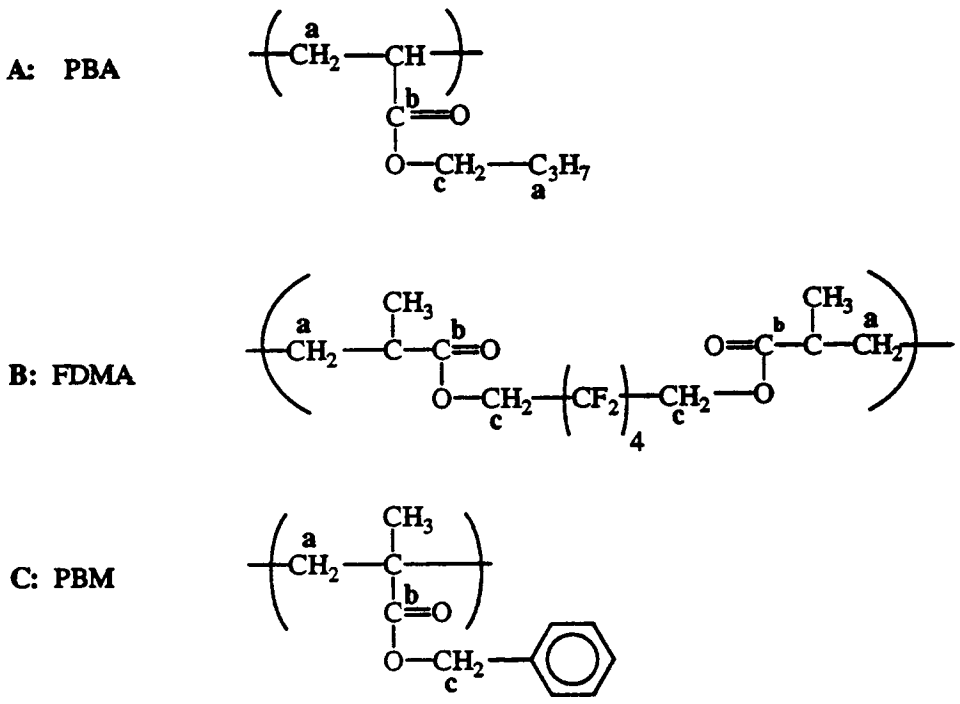

Figure 7 Chemical structure of (A) BA, (B) FDMA, and (C) PBM, depicting the different types of carbon atoms present in the system.

PBM weight ratio. Samples 222, 223, and 226 have similar areas for both peaks agreeing with the approximately 1 : 1 weight ratio of core to shell material. The slightly higher than expected T_{g1} values for samples 224 and 225 are attributed to glassy polymer diffused into the rubbery domains, achieving a certain degree of miscibility or grafting.

Samples of structured latex particles with higher core–shell ratios, namely 252, 253, 261, and 264 were also subjected to DSC tests. Only a low T_g was observed for all four samples. There was no clear indication, however, for the presence of a second, higher T_g. It was difficult to determine the exact value of the second T_g, corresponding to the glassy, second-stage polymer because of the relatively very

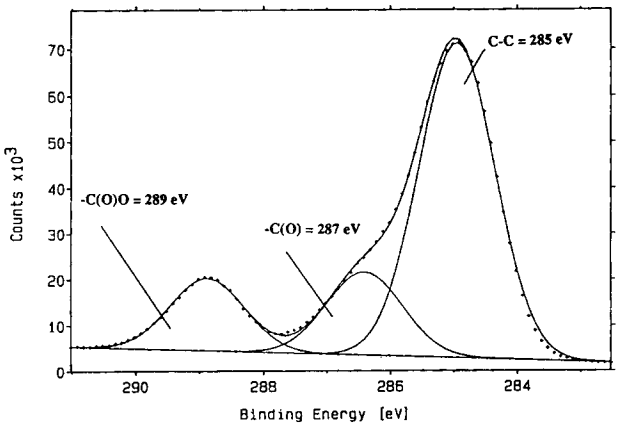

Figure 8 X-ray photoelectron spectra of carbon [C(1s)] peak for a core–shell latex system, indicating the shift in binding energy due to oxygen bonding.

Table X ESCA of Carbon–Oxygen Bearing Carbon (C/CO) Ratios of PBA–FDMA Seed and Structured Latex Particles of Thin and Thick PBM Shell

Theoretical			
	PBA	FDMA	PBM
C/CO	2.5	2.5	4.5
Seed			
C/CO	2.3		
Structured Latex Particles with Thin Shell			
Process	Batch	Semi + CTA	Semi
C/CO	3.3	2.0	2.0
Structured Latex Particles with Thick Shell			
Process	Batch	Semi + CTA	Semi
C/CO	3.6	2.8	2.1

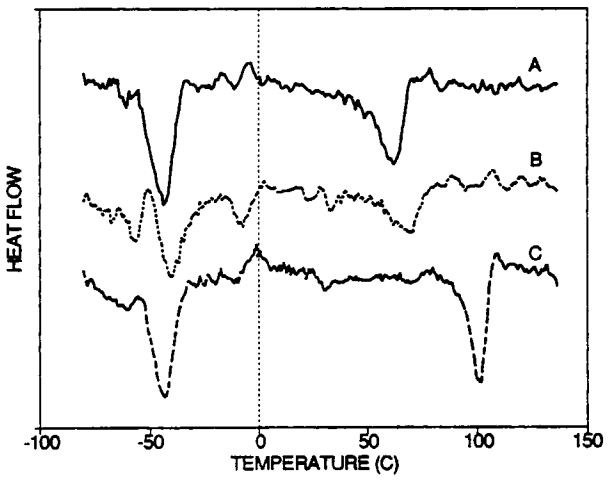

Figure 9 Effect of shell composition on the glass transition temperatures. (A) PBA/PBM, (sample 223), (B) PBA/P(BM–St) (sample 225), and (C) PBA–polystrene (sample 226).

small amount of the shell material. The inflection of the curve at the high range temperatures for the DSC plots was within the noise range of the instrument.

The low-temperature T_g's are tabulated in Table XII as a function of seed particle size and core–shell weight ratio. No significant differences are observed among the T_g's of the various samples.

Dynamic Mechanical Thermal Analysis (DMTA) Studies

In an attempt to better understand the morphology of structured latex particles DMTA tests[49–51] were run on a Polymer Labs DMTA, conditions are specified elsewhere.[46] All samples exhibited a single tan δ maxima, corresponding to the T_g of PBA seed. Any other transitions were below the sensitivity range of the instrument and could not be detected. The tan δ temperatures (T_g) are listed in the last column of Table XII. The results obtained from DMTA analysis follow the same trend as the T_g values obtained from DSC analysis. The temperature differences between the glass transition temperatures of samples comprised of different core–shell ratios and/or different seed particle sizes are too small to allow any correlation between T_g and particle morphology. The shift of about 20°C to higher temperature observed when comparing DMTA analysis with DSC scanning is most probably due to the frequency of the experiment. On the molecular level, the chains are being stressed during the DMTA test and need more time (temperature) to enable relaxation and molecular motion.

Appearance of Freeze-Dried Samples

Table XIII depicts the 230-series compositions and core–shell ratios of the structured latex particles which were freeze dried. Figure 10 is a picture of some of the freeze-dried structured latex samples. Samples 230 [Fig. 10(A)] and 231 [Fig. 10(B)], prepared with 7 and 1 wt % crosslinked PBA seeds, respectively, with a core–shell ratio of 1/3, dried into a powdery material possessing a certain iridescence. The iridescence is an indication of a narrow particle size distribution. Samples 232 [Fig. 10(C)] and 233 with 7 and 1 wt % crosslinker, respectively, and with

Table XI Glass Transition Temperatures (T_g) for Seeds and Structured Latex Particles (First Series of PBA–PBM Latex Particles)

Sample	Seed Type	Shell Composition	T_{g1} (°C)	T_{g2} (°C)	T_g Intermediate
Seed particles					
108	7% crosslinked	−40	—	—	—
109	1% crosslinked	−45	—	—	—
Structured particles					
220	108	100 BM	−40	61	—
221	109	100 BM	−44	62	—
222	108	100 BM	−38	61	—
223	109	100 BM	−44	61	—
224	109	95/5[a] BM–St	−40	67	yes
225	109	95/5[b] BM–St	−39	70	yes
226	109	100 St	−43	101	—

[a] 1.0 wt % IOMP based on BM monomer.
[b] 0.7 wt % IOMP based on BM monomer.

Table XII Glass Transision Temperatures (T_g) Determined by DSC and DMTA for Structured Latex Particles

Sample	Seed Size	Core–Shell Wt Ratio	T_g (°C) (DSC)	T_g (°C) (DMTA)
261	Large	1/0.060	−50	−25
264	Large	1/0.357	−47	−24
252	Small	1/0.435	−48	−23
253	Small	1/0.435	−46	−22

1/1 core–shell ratio, had a more flaky appearance when dried, due to the thinner shell (i.e., a lesser amount of glassy material). Samples 234 [Fig. 10(D)] and 235, prepared with the 1 wt % crosslinked PBA seed at a 1/1 core–shell weight ratio with a shell composition of 95/5 BM–St copolymer also resulted in a flaky appearance of the dried sample. Sample 236 [Fig. 10(E)], with the same core–shell ratio as samples 232–235, with a 1% crosslinked PBA seed and 100% PS shell yielded a cakelike dried material. A transverse cut of this cakelike material reflected a close-packed flaky consistency. A correlation of the freeze-dried appearance with the morphology of the samples (see Fig. 2) indicates that the lower the coverage of the PBA seed surface by the glassy second-stage polymer, the more rubbery and less powdery is the appearance of the freeze-dried material.

SUMMARY AND CONCLUSIONS

Transmission electron micrographs of the latex particles obtained after consecutive polymerization stages indicate the formation of structured latex particles and the absence of a second crop of particles, i.e., all of the second-stage monomer had polymerized onto or into the existing PBA seed latex particles.

Preferential staining coupled with TEM examination showed that the morphology of the structured latex particles is affected by the monomer addition mode, the second-stage monomer composition and amount, as well as the presence of chain transfer agent. A tendency to have a better coverage of the seed latex particle was observed when shifting the second-stage monomer addition mode from batch to semicontinuous feed under starved conditions. This effect results from the interplay of thermodynamic and kinetic factors, where thermodynamic equilibrium strives toward lower free energy levels at the interfaces of the three-phase system (polymer 1, polymer 2, and water), while kinetic factors such as diffusion of the second-stage polymer chains are limited by the viscosity increase at higher molecular weights.[30]

The increase in the amount of second-stage monomer appears to increase the degree of coverage of the seed particles, indicating that there is no complete phase separation between the PBA and the PBM and that at a sufficiently high amount of the second-stage full coverage may be achieved.

The second-stage composition also affects the morphology. PBM leads to better coverage of PBA seed particles than polystyrene does.

The presence of CTA is highly influential on the morphology of the structured latex particles. In the presence of a chain transfer agent, polymer chains are shorter and have higher mobility so they overcome the kinetic barrier, diffusing, and leading to an increased degree of phase separation, resulting in lower free energy levels. In the absence of a chain transfer agent, second-stage polymer chains are of high molecular weight and viscosity, and are less selective as to the polymerization loci. Transmission electron micrographs reveal patches of second-stage polymer spread throughout the PBA seed surface. These patches are observed only for thin-shelled particles, when the amount of second-stage monomer introduced into the system is low.

Glass transition determination of structured latex particles at low core–shell ratios (thick shell) indicate the existence of two distinct phases, a lower glass transition temperature corresponding to the glass transition temperature of the seed (with no shift), and a higher glass transition temperature due to the corresponding composition of the second-stage polymer. Small domains of polymer miscibility or grafting between the seed and the shell material appear to be present, as indicated by some intermediate T_g values. Neither DSC nor DMTA scans

Table XIII Compositions and Core–Shell Weight Ratios for the 230 Series of Structured Latexes

Sample	Seed % Crosslinker	Shell Composition	Core–Shell Ratio
230	7	100 PBM	1/3
231	1	100 PBM	1/3
232	7	100 PBM	1/1
233	1	100 PBM	1/1
234	1	95/5 P(BM–St)[a]	1/1
235	1	95/5 P(BM–St)[b]	1/1
236	1	100 PS	1/1

[a] 1.0 wt % IOMP based on second-stage monomer.
[b] 0.7 wt % IOMP based on second-stage monomer.

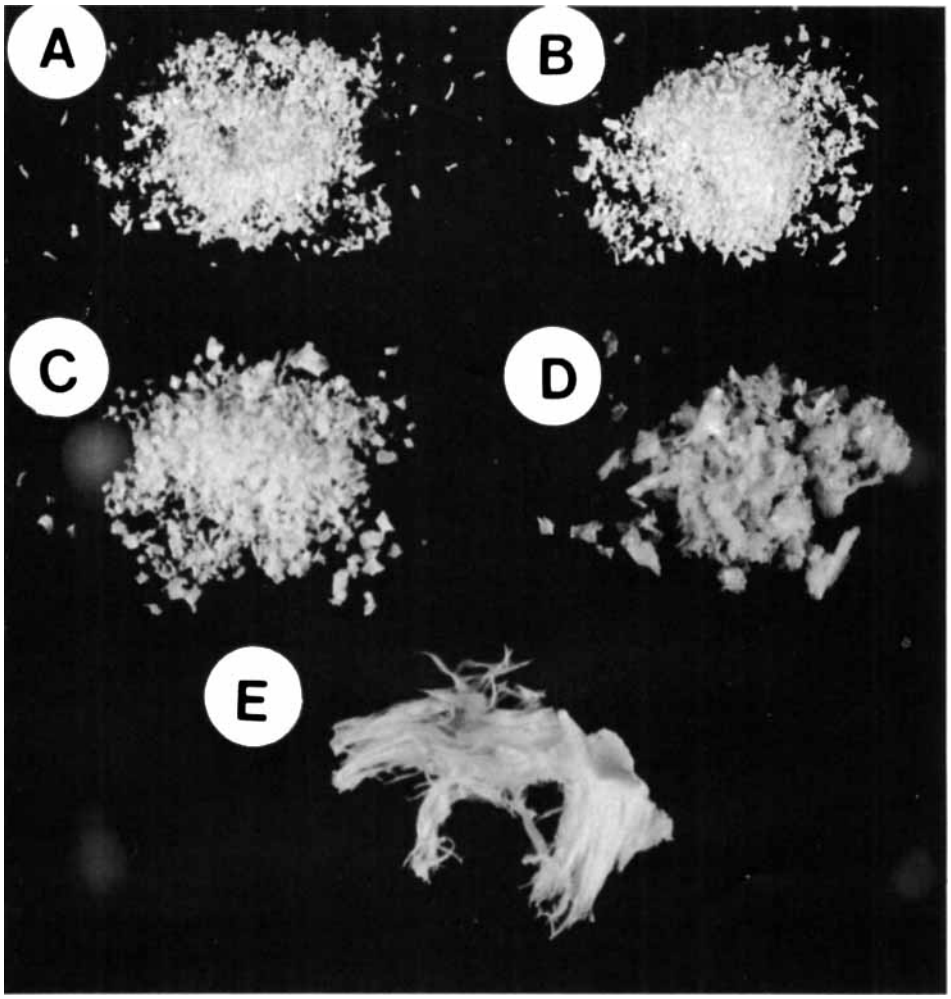

Figure 10 Freeze-dried structured (core–shell) latex particles; seed particle diameter = 180 nm. (A) PBA seed (7% crosslinker), PBM shell (calculated 50 nm); (B) PBA seed (1% crosslinker), PBM shell (calculated 50 nm); (C) PBA seed (7% crosslinker), PBM shell (calculated 25 nm); (D) PBA seed (1% crosslinker), 95/5 P(BM–St) shell wt ratio (calculated 25 nm); and (E) PBA seed (1% crosslinker), PS shell (calculated 25 nm).

of high core–shell ratios (thin shells), where the second-stage polymer content is low, can detect the presence of the second-stage polymer and determine its T_g.

The authors wish to thank Olga Shaffer for her invaluable help with electron microscopy techniques and EniChem America Inc. for partial support of this work.

REFERENCES

1. W. D. Hergeth and K. Schmutzler, *Acta Polym.*, **36,** 472 (1985).
2. S. L. Rosen, *J. Appl. Polym. Sci.*, **17,** 1805 (1973).
3. V. Dimonie, M. S. El-Aasser, A. Klein, and J. W. Vanderhoff, *J. Polym. Sci.: Polym. Chem. Ed.*, **22,** 2197 (1984).
4. M. Okubo, *Makromol. Chem. Macromol. Symp.*, **35,** 307 (1990).
5. I. Cho and K-W Lee, *J. Appl. Polym. Sci.*, **30,** 1903 (1985).
6. D. I. Lee and T. J. Ishikawa, *Polym. Sci. Polym. Chem. Ed.*, **21,** 147 (1983).
7. Y. Nakamura, H. Tabata, H. Suzuki, K. Iko, M. Okubo, and T. Matsumoto, *J. Appl. Polym. Sci.*, **32,** 4865 (1986).
8. Y. Nakamura, H. Tabata, H. Suzuki, K. Iko, M. Okubo, and T. Matsumoto, *J. Appl. Polym. Sci.*, **33,** 885 (1987).
9. D. C. Sundberg and M. R. Muscato, *J. Appl. Polym. Sci.*, **41,** 1425 (1990).

10. M. Okubo, A. Yamada, and T. Matsumoto, *J. Polym. Sci. Polym. Chem. Ed.*, **16,** 3219 (1980).
11. M. Okubo, M. Ando, A. Yamada, Y. Katsuta, and T. Matsumoto, *J. Polym. Sci., Polym. Lett. Ed.*, **19,** 143 (1981).
12. M. Okubo, Y. Katsuta, and T. Matsumoto, *J. Polym. Sci., Polym. Lett. Ed.*, **18,** 481 (1980).
13. M. Okubo, Y. Katsuta, and T. Matsumoto, *J. Polym. Sci., Polym. Lett. Ed.*, **20,** 45 (1982).
14. D. R. Stutman, A. Klein, M. S. El-Aasser, and J. W. Vanderhoff, *Ind. Engr. Chem. Prod. Res. Dev.*, **24,** 404 (1985).
15. D. Sundberg, A. P. Casassa, J. Pantazopoulos, M. R. Muscato, B. Kronberg, and J. Berg, *J. Appl. Polym. Sci.*, **45,** 1425 (1990).
16. M. R. Grancio and D. J. Williams, *J. Polym. Sci.*, **8,** 2617 (1970).
17. D. J. Williams, *Polym. Prepr.*, **12,** 464 (1971).
18. P. Keusch and D. J. Williams, *J. Polym. Sci. Polym. Chem. Ed.*, **11,** 143 (1973).
19. A. Garcia-Rejon, L. Rios, and L. A. Lopez-Latorre, *Polym. Eng. Sci.*, **27,** 463 (1987).
20. Y-C. Chen, Ph.D. Dissertation, Lehigh University, 1991.
21. Y. C. Chen, V. L. Dimonie, and M. S. El-Aasser, *J. Appl. Polym. Sci.*, **42,** 1049 (1991).
22. Y. C. Chen, V. L. Dimonie, and M. S. El-Aasser, *J. Appl. Polym. Sci.*, **45,** 487 (1992).
23. Y. C. Chen, V. L. Dimonie, and M. S. El-Aasser, *Macromolecules*, **24,** 3779 (1991).
24. M. R. Muscato and D. C. Sundberg, *J. Polym. Sci.: Part B: Polym. Phys.*, **29,** 1021 (1991).
25. J. Berg, D. Sundberg, and B. Kronberg, *Polym. Mat. Sci. Eng.*, **54,** 367 (1986).
26. J. Berg, D. Sundberg, and B. Kronberg, *J. Microencap.*, **6,** 327 (1989).
27. L. Jansson, H. Nilsson, C. Sivegren, and B. Tornell, *Thermochim. Acta*, **118,** 97 (1987).
28. T. Hamazaki, Y. Kanchiku, R. Handa, and M. Izumi, *J. Appl. Polym. Sci.*, **21,** 1569 (1977).
29. S. Y. Hobbs, M. E. J. Dekkers, and V. H. Watkins, *Polymer*, **29,** 1598 (1988).
30. S. Lee and A. Rudin, in *Polymer Latexes, Preparation, Characterization, and applications*, E. S. Daniels, E. D. Sudol, and M. S. El-Aasser, eds., ACS Symposium Series 492, Am. Chem. Soc., Washington D.C., 1992.
31. D. Beyer, W. Lebek, W.-D. Hergeth, and K. Schmutzler, *Colloids Polym. Sci.*, **268,** 744 (1990).
32. W. D. Hergeth, K. Schmutzler, and S. Wartewig, *Makromol. Chem. Macromol. Symp.*, **31,** 123 (1990).
33. D. I. Lee, in *Emulsion Polymers and Emulsion Polymerization*, D. R. Bassed and A. E. Hamielec, Eds., ACS Symp. Ser., 165, Washington, D.C., **165,** 405 (1981).
34. G. Kanig and H. Neff, *Colloid Polym. Sci.*, **253,** 29 (1975).
35. S. C. Misra, C. Pichot, M. S. El-Aasser, and J. W. Vanderhoff, *J. Polym. Sci., Polym. Lett. Ed.*, **17,** 567 (1979).
36. D. Distler and G. Kanig, *Colloid Polym. Sci.*, **256,** 1052 (1978).
37. D. Distler and G. Kanig, *Organic Coat. Plast. Chem.*, **4,** 606 (1980).
38. W. Brouwer, *Coll. Surf.*, **40,** 235 (1989).
39. P. Cebeillac, M-J Fauran-Clavel, C. Lacabanne, and J. P. Ibar, *Polymeric Materials Science and Engineering, Proceedings of the ACS Division of Polymeric Materials Science and Engineering*, ACS Books and Journals Division Pub., Washington, D.C., **60,** 855, 1989.
40. G. E. Molau, *J. Polym. Sci. Part A*, **3,** 4235 (1965).
41. G. E. Molau, *J. Polym. Sci. Part A*, **3,** 1267 (1965).
42. Y. Ikada, F. Horii, and I. Sakurada, *J. Polym. Sci., Polym. Chem. Ed.*, **11,** 27 (1973).
43. F. Horii, Y. Ikada, and I. Sakurada, *J. Polym. Sci., Polym. Chem. Ed.*, **11,** 41 (1973).
44. H. A. J. Battaerd and G. W. Tregrear, *Graft Copolymers*, Wiley, New York, 1967.
45. T. I. Min, A. Klein, M. S. El-Aasser, and J. W. Vanderhoff, *J. Polym. Sci., Polym. Chem. Ed.*, **21,** 10 (1983).
46. I. Segall, Ph.D. Dissertation, Lehigh University, 1992.
47. D. T. Clark, in *Polymer Surfaces*, D. T. Clark and W. J. Feast, Eds., Wiley, New York, 1978.
48. A. Arora, M.S. Report, Lehigh University, 1992.
49. L. H. Sperling, *Introduction to Physical Polymer Science*, Wiley, New York, 1986.
50. F. Rodriguez, *Principles of Polymer Systems*, 2nd ed., McGraw-Hill, New York, 1982.
51. J. J. Aklonis, W. J. MacKnight, and M. C. Shen, *Introduction to Polymer Viscoelasticity*, Wiley, New York, 1972.

Received September 12, 1994
Accepted November 16, 1994